

From full-scale testing of steel lattice towers to stochastic reliability analysis

J. SZAFRAN, M. KAMIŃSKI

*Chair of Structural Reliability
Department of Structural Mechanics
Faculty of Civil Engineering, Architecture
and Environmental Engineering
Łódź University of Technology
Al. Politechniki 6
90-924 Łódź, Poland
e-mail: Marcin.Kaminski@p.lodz.pl*

THIS WORK IS FOCUSED on the experimental-based Stochastic Finite Element Method analysis of the steel lattice telecommunication structure exposed to the wind pressure, whose average value is treated as the Gaussian random variable. The Least Squares Method is provided here for symbolic recovery of the polynomial responses of this structure in addition to the given uncertainty source and it serves to the twentieth order perturbation-based approximations for the first four probabilistic moments and coefficients. Static numerical analysis has been carried out by the use of the incremental BFGS (Broyden–Fletcher–Goldfarb–Shanno) procedure necessary for the so-called P-delta effect in steel structures, while the basic statistics of the ultimate limit state have been included into the formulas for the reliability indices of both first and second order. This study shows that the safety margin of such structures is definitely wider than it follows the basic Eurocodes statements, which means that designed durability period for these telecommunication structures is definitely longer.

Key words: Stochastic Finite Element Method, full-scale experiment, lattice structures, reliability analysis, geometrical nonlinearity.

Copyright © 2017 by IPPT PAN

1. Introduction

IT IS WIDELY KNOWN that the wind pressure and its dynamical excitation is a very important environmental action on various engineering structures [1], which becomes decisive for the stability and capacity of the skeletal steel and aluminum communication structures [2]. The effect of the wind on the tower structures has been studied many times in the literature including both experimental and numerical methods [3–5]. A specific subject of such analyses were aerodynamic damping of various cross-sections, horizontal deflections as well as the effective static loads replacing real dynamic excitation of the winds [6, 7].

A real problem with telecommunication towers is that these structures are relatively new and there is no rich evidence concerning their failures in engineering literature unlike for the transmission towers [8], also in testing phase [9]. This evidence has limited importance for the telecommunication towers, because the wind pressure is dominating, while transmission towers are subjected to a combination of the wind and ice covers. Let us note that the wind induced dynamic excitations have been extensively studied including dynamic instabilities as well as fatigue effects and collapses of various vertical slender structures [10–12]. There is no doubt that realistic analysis of the bearing capacity and stability of the towers needs some full scale tests and these scarce experiments were reported in [13–15], where traditionally nonlinear static analysis [16] is preferred instead of the dynamical response of the towers. It is also known that uncertainty and stochasticity is an inherent part of the wind loading – this aspect has been studied initially by the traditional crude Monte-Carlo sampling in terms of complex structures [17], further focused on reliability issues of the towers themselves [18]. This technique has been replaced later with importance sampling while minimizing the computer effort and overall simulation time [19], while recently have been replaced with the stochastic perturbation technique allowing for eigenvalue [20] and stability analysis [21] for the telecommunication towers. This technique is fast, accurate and does not demand massive computers and it originates from the Second Order Second Moment (SOSM) version [22], where the expectations and variances are determined. However, recently its generalized modification to the n th order Taylor expansion [23] became popular due to larger accuracy and computer algebra implementations which enables for an efficient computation of the skewness and kurtosis of the state functions also. Its further implementations may obey stochastic dynamic effects in the skeletal tower and mast structures, similarly to numerical studies contained in [24, 25].

A majority of this study is in presentation of the push-over test in a form of the breaking force and buckling resistance of the tower and further direct application of these data into Stochastic Finite Element Method (SFEM) reliability analysis of this tower according to both First and Second Order Reliability Methods (FORM & SORM). Following previous computational models [13, 16] we apply geometrically nonlinear static analysis to detect extreme normal force serving for the Ultimate Limit State (ULS). It is important to notice that the dominating design variable in the skeletal structures, i.e., the characteristic wind pressure, is considered here as the Gaussian random parameter with the given expectation and some variability interval for the coefficient of variation. It is known [26] that the wind pressure field for tall buildings has non-Gaussian character, however due to remarkably smaller height of the transmission towers and its slenderness with the few orders larger than for the buildings, numerical modelling of the wind speed as the Gaussian PDF is well justified. It is true that the

applied version of the Stochastic Finite Element Method permits non-Gaussian variables, but neither existing literature nor the engineering codes do not contain sufficient information, so that Gaussian PDF has been adopted after Central Limit Theorem. Further, the wind is modeled physically as the Newtonian, viscous fluid, whose non-turbulent flow with no pressure gradient is replaced with its static equivalent; some other models with Finite Volume Method (FVM) for the fluid flow part and Finite Element Method (FEM) for the structural analysis could overcome these limitations (i.e., by solving fluid-solid stochastic interaction problem). The generalized stochastic perturbation method of the higher order is implemented with the FEM program Autodesk ROBOT Structural Analysis v. 2015 [27] to calculate the first four probabilistic moments and characteristics of the given state parameter. Higher order expansions have been programmed in the computer algebra program MAPLE v. 2016 [28] together with the Least Squares Method recovery of the extreme normal force polynomial response function. It is theoretically and numerically demonstrated that the proposed stochastic technique is efficient in modeling of geometric nonlinearities subjected to random loadings, while the principal engineering outcome is that the realistic capacity of the steel tower structures is higher than it follows the basic statements of the Eurocodes [29].

2. Structural experiment description

The tower has been manufactured as a three-dimensional beam structure with the rebars having a horizontal square cross-section, the height equal to 42.0 m (see Fig. 1) and has been divided into seven sections. This tower has a linear convergence of the legs for the first six sections (up to 36 above the terrain level, while the highest section has a form of the prism with the diameter equal to 0.90 m. The legs of the tower has been manufactured by using of the circular hollow sections (sizes from 114.3 mm \times 6.3 mm to 60.3 mm \times 3.6 mm). The diagonal bracing members have been designed as circular and rectangular hollow sections as well as the channel bars. All structural elements have been manufactured with the structural steel S 355. All the connections in-between fundamental structural elements of the tower (legs and the rebars) have been manufactured in lower sections (S-3–S-7) with the use of plates and bolts (a single per a joint – rotation admissible), while two upper segments (S-1–S-2) have been completely welded (fully stiff). The X rebars pattern has been applied within the segments S-4 do S-7, while the segments from S-1 to S-3 have K pattern. The rebars are discontinuous from the leg to leg – they are connected with each other in the crossing at the half of a distance in-between the legs being connected. A continuity of the legs throughout their lengths is assured by the bolted joints in the circular plates finishing each section.



FIG. 1. The general view of the tower (top left), failure mode of the leg in the lowest section (top right and bottom).

The main objectives of this experiment were:

- an identification of the failure mechanism and failure mode,
- measurements of strains in the tower legs,
- determination of the breaking external load, which can be assumed as a structure experimental load capacity.

The hardware engaged to accomplish these goals included measurement equipment capable of the strains notification for all the tower members (a load cell allowing for a direct registration of strain and external load values), of the geodetic displacement measurements, and of the video registration of the structure be-

havior under the ultimate load. This study is focused on the values of axial forces in the tower legs, the failure mechanism of the structure, and the displacements of the joints observed during the pushover test.

The geometrical scheme of the entire tower adopted further in the FEM simulations have been shown in Fig. 2, whereas the full specification of the structural steel profiles is included in Table 1.

Table 1. Selected tower members steel profiles.

Section	Height of the section [m]	Legs steel profiles types	Diagonal bracing steel profiles types
S-1	6.0	CHS 60.3 × 3.6	Ø22
S-2	6.0	CHS 70.0 × 4.0	RHS 25.0 × 3.0
S-3	6.0	CHS 76.1 × 5.0	CHS 38.0 × 4.0
S-4	6.0	CHS 88.9 × 6.3	C 30 × 30 × 3
S-5	6.0	CHS 88.9 × 6.3	C 30 × 30 × 3
S-6	6.0	CHS 114.3 × 6.3	C 40 × 40 × 3
S-7	6.0	CHS 114.3 × 6.3	C 40 × 40 × 3

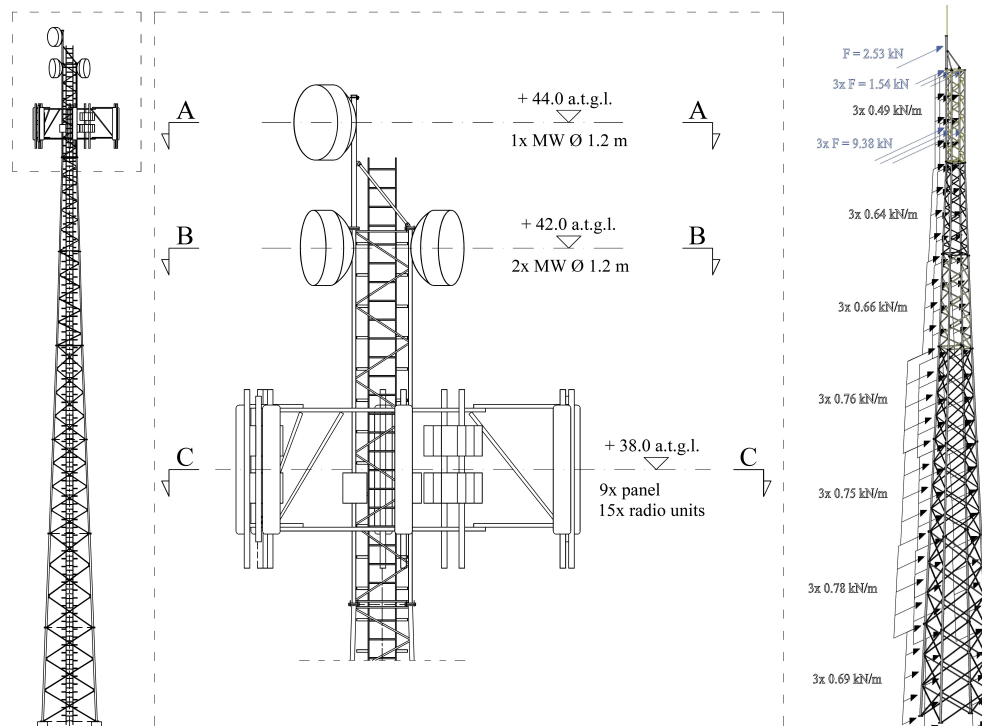


FIG. 2. Scheme of the tested tower with telecommunication equipment (left) and the wind pressure distribution (right) taken to the reliability analysis.

A general view of the pushover experiment in the vertical plane has been presented in Fig. 3, where a towing truck applying the external force through the steel wire cable on the tower structure is shown. Application of this force has also incremental character similarly to further computer FEM simulations. We need to mention that the main motivation of this specific static scheme was to simulate experimentally an influence of the wind pressure on this structure. Unfortunately, due to the technical limitations (a limited area of the experiment) it was unable to assure a smaller angle of application of the concentrated force (specifically in the horizontal direction), while its attachment point is equivalent to the location of the effective concentrated force coming from the overall wind pressure. The basic experimental results are obtained as the overall breaking force value of 113.2 kN and the experimental buckling resistance of the tower leg, whose buckled deformed configuration is given in Fig. 1, also – 753.3 kN. It is very important to mention that both values are remarkably larger than their Eurocode counterparts, which validates designing codes procedures. The smaller value from these two is taken as the mean resistance during calculation of the reliability indices during the SFEM experiments.

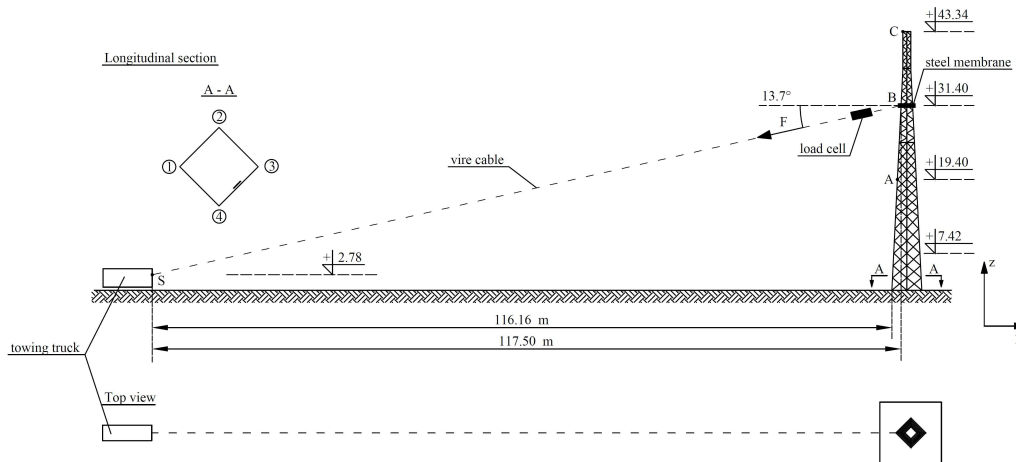


FIG. 3. Full static scheme of the pushover tower.

Further, various computer models of the same tower have been tested to obtain the best fitting into the failure process and have been all prepared with the use of FEM civil engineering system Autodesk ROBOT Structural Analysis v. 2015 according to its wide availability and free student licenses. The failure mechanism itself, the failure form and the entire uploading process may be seen online (cf. [30]). Model 1 has been built with the use of 222 3D linear beam finite elements connected in 278 nodal points, where all structural connections

– in-between the legs sections as well as in-between the legs and rebars (two bolts of the class 8.8) have been set as completely rigid. Additionally, the geometrical imperfections have been added to the legs in two lower segments (S-7 and S-6) that have been measured before the experiment – these are about 15 mm for the legs in S-7 as well as about 8.0 mm in the section S-6. These initial deformations have been noticed in the mid-span of these elements, so that in a location of the gusset plates (see Fig. 2 (right)) and their computational implementation has been made by replacing perfect geometry with adding new finite elements fitting curvilinear deformed shape in-between the original nodes; therefore, the resulting displacements are given in addition to the original geometry. Finally, compatible nodes have been inserted in all the crossings within the X patterns of the tower rebars. Model 2 is an extension of Model 1 by an application of the elastic supports (connections with the foundation). The compliance coefficient has been detected on the basis of real displacements of the supporting nodes for the uploading level 125.0 kN, for each support independently. Model 3 includes all the features of Model 2, but additionally geometrically nonlinear analysis has been performed (the so-called P- Δ analysis) according to the BFGS (Broyden–Fletcher–Goldfarb–Shanno) algorithm. The resulting relations in-between external force and displacements of points A and C together with some experimental evidence have been presented in Fig. 4. As one can notice, Model 3 returns the results very close to each other. Observation of the experimental data (green curves) are in agreement with the stability theory for large systems with geometrical imperfections where the displacements increase significantly and nonlinearly when approaching the value of breaking load. Test and computational results are consistent within the range of external load up to approx. 100 kN. It has been decided that this convergence is good enough for further reliability analysis.

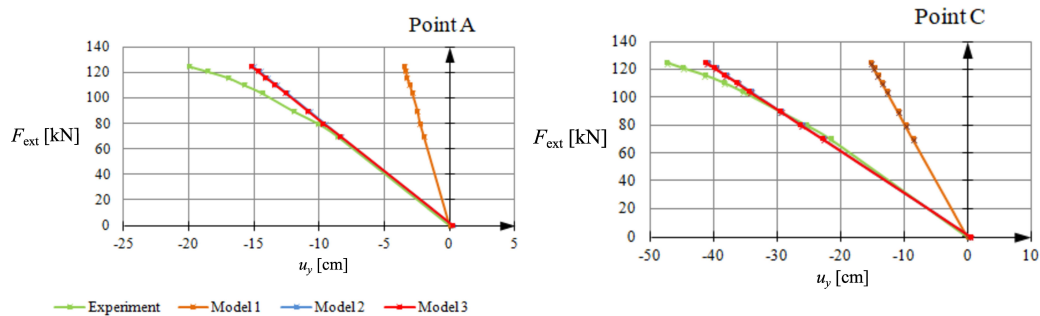


FIG. 4. Various FEM models of the pushover experiment.

3. Stochastic perturbation technique in reliability analysis

The generalized stochastic perturbation technique is based on an expansion of all the random functions into the Taylor series of the required order. In this particular formulation, assumptions of the Gaussian probability density function is not necessary, because we can implement such an approach to the non-symmetrical density distribution as well. Such an expansion applied for the sought random deflection u resulting from the uncertain wind velocity $\nu(\omega)$ can be expanded as

$$(3.1) \quad u(\nu(\omega)) = u^0(\nu^0(\omega)) + \varepsilon \left. \frac{du(\nu(\omega))}{d\nu} \right|_{\nu=\nu^0} \Delta\nu + \dots + \frac{\varepsilon^n}{n!} \left. \frac{d^n u(\nu(\omega))}{d\nu^n} \right|_{\nu=\nu^0} \Delta\nu^n$$

and classical integral definitions like these adjacent for the M th central probabilistic moments

$$(3.2) \quad \mu_M(u(\nu)) = \int_{-\infty}^{+\infty} (u(\nu) - E(u(\nu)))^M p_{u(\nu)}(x) dx.$$

A full symbolic approach guarantees the expansion with a priori given length and its *a posteriori* modifications according to the numerical errors obtained for higher than the second probabilistic moments of the structural deformations. The method in the structural context is based on the iterative solution of the discrete equilibrium equation

$$(3.3) \quad \Delta K_{\alpha\beta}^{\Delta} q_{\beta} = \Delta Q_{\alpha}$$

using the Broyden–Fletcher–Goldfarb–Shanno (BFGS) [31, 32] strategy to get the series of deterministic nodal responses increments Δq_{β} . Application of the Taylor expansion in this problem is less complicated than structural problems with randomized material characteristics, because all derivatives of the stiffness matrix with respect to the input random variables vanishes, while the R.H.S. (Right Hand Side) vector exhibits zeroth and the first order terms only in stochastic expansions as higher than the first order derivatives to random ν vanish also. Let us start from an incremental formulation of the FEM equations and their stochastic counterparts using an additional local polynomial basis of the given order. We obtain the following polynomial representations for the state functions:

- for the structural displacements increments as

$$(3.4) \quad \Delta u_{\zeta} = a_{\zeta\beta} \Delta q_{\beta} = a_{\zeta\beta} D_{\beta}^{(p)} \nu^p, \quad p = 0, \dots, n-1, \quad \beta, \zeta = 1, \dots, N;$$

- increments of the strain tensor components

$$(3.5) \quad \Delta \varepsilon_{kl} = \Delta \bar{\varepsilon}_{kl} + \Delta \bar{\bar{\varepsilon}}_{kl} = \bar{B}_{kl}^{\zeta} a_{\zeta\alpha} D_{\alpha p} b^p + \bar{\bar{B}}_{kl}^{\zeta\xi} a_{\zeta\alpha} D_{\alpha p} b^p a_{\xi\beta} D_{\beta r} b^r, \\ p, r = 0, \dots, n-1, \quad \alpha, \beta = 1, \dots, N, \quad k, l = 1, 2, 3;$$

- increments of the second Piola-Kirchhoff stress tensor as

$$(3.6) \quad \Delta \tilde{\sigma}_{ij} = C_{ijkl} \Delta \varepsilon_{kl} = C_{ijkl} (\bar{B}_{kl}^{\zeta} a_{\zeta\alpha} D_{\alpha p} \nu^p + \bar{\bar{B}}_{kl}^{\zeta\xi} a_{\zeta\alpha} D_{\alpha p} \nu^p a_{\xi\beta} D_{\beta r} \nu^r), \\ p, r = 0, \dots, n-1, \quad \alpha, \beta = 1, \dots, N, \quad i, j, k, l = 1, 2, 3.$$

Partial derivatives of these state functions with respect to the parameter b are derived analytically and are used in determination of the structural response probabilistic moments. There holds:

- for the first partial derivatives of the displacements

$$(3.7) \quad \frac{d\Delta u_{\zeta}}{d\nu} = a_{\zeta\beta} \frac{d\Delta q_{\beta}}{d\nu} = a_{\zeta\beta} \frac{d(D_{\beta}^{(p)} \nu^p)}{d\nu} = p a_{\zeta\beta} D_{\beta}^{(p)} \nu^{p-1}, \\ p = 0, \dots, n-1, \quad \beta = 1, \dots, N,$$

- as well as for analogous m th order derivatives

$$(3.8) \quad \frac{d^m \Delta u_{\zeta}}{d\nu^m} = a_{\zeta\beta} \frac{d^m \Delta q_{\beta}}{d\nu^m} = a_{\zeta\beta} \frac{d^m (D_{\beta}^{(p)} \nu^p)}{d\nu^m} = p \dots (p-m) a_{\zeta\beta} D_{\beta}^{(p)} \nu^{p-m}, \\ p = 0, \dots, n-1, \quad \beta = 1, \dots, N.$$

Further, we determine the strain tensor components partial derivatives with respect to the input random variable ν as

$$(3.9) \quad \frac{d\Delta \varepsilon_{kl}}{d\nu} = \bar{B}_{kl}^{\zeta} a_{\zeta\alpha} p D_{\alpha p} \nu^{p-1} + \bar{\bar{B}}_{kl}^{\zeta\xi} a_{\zeta\alpha} D_{\alpha p} p \nu^{p-1} a_{\xi\beta} D_{\beta r} \nu^r \\ + \bar{\bar{B}}_{kl}^{\zeta\xi} a_{\zeta\alpha} D_{\alpha p} \nu^p a_{\xi\beta} D_{\beta r} r \nu^{r-1}, \quad p, r = 0, \dots, n-1, \quad \beta = 1, \dots, N, \quad k, l = 1, 2, 3.$$

Let us note that polynomial basis degree is a subject of the separate optimization – it maximizes a correlation of this basis to the FEM trial points and minimizes mean square error of such an approximation. The local character of this basis shows variations of such an optimal degree in-between different degrees of freedom in the FEM model. Further determination of the probabilistic moments proceeds from their integral definitions extracted from Eq. (3.2) thanks to the symbolic derivation of all partial derivatives with respect to the given random input variable ν . There holds for the expected values of the force F

$$\begin{aligned}
(3.10) \quad E[F(\nu)] &= F^0(\nu^0) + \frac{1}{2} \frac{d^2 F(\nu)}{d\nu^2} \mu_2(\nu) \\
&+ \frac{1}{4!} \frac{d^4 F(\nu)}{d\nu^4} \mu_4(\nu) + \frac{1}{6!} \frac{d^6 F(\nu)}{d\nu^6} \mu_6(\nu) \\
&+ \frac{1}{8!} \frac{d^8 F(\nu)}{d\nu^8} \mu_8(\nu) + \frac{1}{10!} \frac{d^{10} F(\nu)}{d\nu^{10}} \mu_{10}(\nu),
\end{aligned}$$

as well as for the variances of the same force inherent in the Ultimate Limit State verification

$$\begin{aligned}
(3.11) \quad \text{Var}(F(\nu)) &= \mu_2(\nu) \left(\frac{dF(\nu)}{d\nu} \right)^2 + \mu_4(\nu) \left\{ \frac{1}{4} \left(\frac{d^2 F(\nu)}{d\nu^2} \right)^2 + \frac{1}{3} \frac{d^3 F(\nu)}{d\nu^3} \frac{dF(\nu)}{d\nu} \right\} \\
&+ \mu_6(\nu) \left\{ \frac{1}{36} \left(\frac{d^3 F(\nu)}{d\nu^3} \right)^2 + \frac{1}{24} \frac{d^4 F(\nu)}{d\nu^4} \frac{d^2 F(\nu)}{d\nu^2} + \frac{1}{60} \frac{d^5 F(\nu)}{d\nu^5} \frac{dF(\nu)}{d\nu} \right\} \\
&+ \mu_8(\nu) \left\{ \frac{1}{576} \left(\frac{d^4 F(\nu)}{d\nu^4} \right)^2 + \frac{1}{360} \frac{d^5 F(\nu)}{d\nu^5} \frac{d^3 F(\nu)}{d\nu^3} + \frac{1}{2520} \frac{d^7 F(\nu)}{d\nu^7} \frac{dF(\nu)}{d\nu} \right. \\
&\quad \left. + \frac{1}{720} \frac{d^6 F(\nu)}{d\nu^6} \frac{d^2 F(\nu)}{d\nu^2} \right\} \\
&+ \mu_{10}(\nu) \left\{ \frac{1}{14400} \left(\frac{d^5 F(\nu)}{d\nu^5} \right)^2 + \frac{1}{40320} \frac{d^8 F(\nu)}{d\nu^8} \frac{d^2 F(\nu)}{d\nu^2} + \frac{1}{8640} \frac{d^6 F(\nu)}{d\nu^6} \frac{d^4 F(\nu)}{d\nu^4} \right\} \\
&+ \mu_{10}(\nu) \left\{ \frac{1}{15120} \frac{d^7 F(\nu)}{d\nu^7} \frac{d^3 F(\nu)}{d\nu^3} + \frac{1}{181440} \frac{d^9 F(\nu)}{d\nu^9} \frac{dF(\nu)}{d\nu} \right\}.
\end{aligned}$$

It is seen that detection of the optimal expansion order is very important considering complexity of the resulting equations and may be provided for each consecutive moment separately. This is the reason, together with numerical efficiency, to use in computational experiments up to the tenth order expansions for expectations and variances, while up to twentieth while analyzing the skewness and kurtosis. All the remaining expansions for the third and fourth central probabilistic moments can be directly found in [23], for non-symmetric probability distributions also.

The first two probabilistic moments of the elongation are determined analytically as the linear transform of the normal force F of the given rebar. This procedure may be necessary for the Ultimate Limit State analysis and it is clear that complex perturbation-based formulas of the twentieth order as above are not necessary here at all. There holds

$$(3.12) \quad \begin{cases} E[\Delta u] = \frac{EA}{L} E[F], \\ \text{Var}(\Delta u) = \frac{E^2 A^2}{L^2} \text{Var}(F), \end{cases}$$

where E , A and L denote Young modulus, a cross-sectional area and the length of this element.

After calculation of the first and second order statistics of the structural response, we proceed with determination of the reliability index, which is the basis to introduce some set of required levels of the structural safety, varying requirements depending on the consequences of a possible failure or object damage. The limit state function can be expressed in case of the tower capacity analysis (with revealed “weakest link”) and random wind load in the following form:

$$(3.13) \quad g = F_{b,ex} - F_x,$$

where F_x is the axial force in a tower leg under compression. The reliability index is defined as a reciprocal of the safety margin according to the First Order Reliability Method. We can express it in the following manner for our case study [33]:

$$(3.14) \quad \beta_{\text{FORM}} = \frac{E[F_{b,ex}] - E[F_x]}{\sqrt{\sigma[F_{b,ex}]^2 + \sigma[F_x]^2}},$$

where $E[F_{b,ex}]$ denotes the expected value of the experimental buckling resistance, $E[F_x]$ is the expected value of the axial forces in a tower leg under compression according to the random wind velocity and $\sigma[F_{b,ex}]$, $\sigma[F_x]$ are standard deviations of both above variables, respectively. The general formula of the reliability index in the Second Order Reliability Method (SORM) applied in further numerical analysis is the following one [33]:

$$(3.15) \quad \beta_{\text{SORM}} = -\Phi^{-1}(P_{f2}),$$

where P_{f2} denotes the probability of failure for the Gaussian probability distribution Φ of the function related to β_{FORM} in the following manner:

$$(3.16) \quad P_{f2} = \frac{\Phi(\beta_{\text{FORM}})}{\sqrt{1 + \beta_{\text{FORM}}\kappa}},$$

where κ stands for a curvature of the limit function g (surface) usually defined as

$$(3.17) \quad \kappa = \frac{\frac{d^2g}{dv^2}}{\left(1 + \left(\frac{dg}{dv}\right)^2\right)^{3/2}}.$$

It is known that FORM reliability analysis recommended in the Eurocodes is not efficient for highly nonlinear limit functions or surfaces, so that a comparison of both approaches is recommended and included in the further numerical section.

4. Computer simulation

Deterministic computer analysis has been carried out with the use of the FEM civil engineering system Autodesk ROBOT Structural Analysis v. 2015, where 383 3D linear beam elements have been provided with 287 nodal points (with 6 d.o.f. each). The tower has fixed elastic supports at the lowest nodes – compressive mode has stiffness set as $K_z = 500\,000$ kN/m, while $K_z = 2\,500\,000$ kN/m in tension. Geometrical imperfections have been defined automatically after Eurocode EC3:2005, buckling coefficients are adopted as 1,0 for all structural members and compatible nodes are provided in all X rebars pattern crossings (the same displacements in each direction and full transfer of the longitudinal force). The nonlinear incremental static solution has been obtained with the algorithm BFGS (relevant to the so-called P- Δ option in this software) with structural matrices automatic update after each increment. The following parameters have been fixed: a number of the increments – 5, a maximum iterations number for a single increment – 40, a number of reductions for the increment length – 3, the reduction coefficient of the increment length – 0,5, a maximum number of ‘line search’ options – 0, control parameter of the ‘line search’ method – 0,5, maximum number of the corrections in BFGS algorithm – 10, a tolerance of the relative norm for the residual forces – 0,0001, a tolerance of the relative norm for the displacements – 0,0001. The wind pressure throughout the tower has been defined according to the Eurocodes [27] too as the non-uniform (height dependent) equivalent static pressure on its structural elements corrected with the aerodynamic coefficient of different cross-sections. The wind pressure distribution and magnitude for a tower body as well as telecommunication equipment and for an expected value of wind velocity is presented in Fig. 1 (right). Numerical recovery of the normal force polynomial response function has been done by 11 repetitions of the same boundary value problem with a varying magnitude of the wind pressure for its about $\pm 50\%$ variations about the mean values; this variability interval has been subdivided into the equidistant discrete values that differ with about 10% from each other. Final results of the extreme normal force have been linked with this magnitude using the Least Squares Method polynomial approximation of the optimal order. This order minimizes the error and variances of LSM fitting and maximizes the cross-correlation in-between the FEM experiments and the target polynomial. This procedure has been entirely implemented in the computer algebra system MAPLE v. 2016, where additionally all the first four probabilistic moments and coefficients have been derived according to the stochastic perturbation technique equations. Finally, the same system served for calculation of both FORM and SORM reliability indices and overall visualization of all the numerical results.

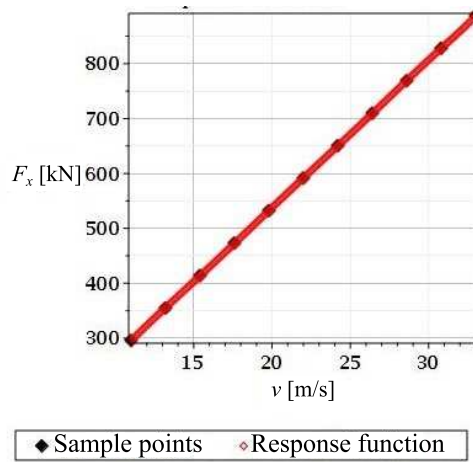


FIG. 5. Response function of the extreme normal force in the tower.

Computational results are contained in Fig. 5 – an extreme normal force response function, while Fig. 6 and 7 illustrating expectation, the coefficient of variation, skewness and kurtosis of this force as the functions of an input coefficient of variation $\alpha(\nu)$. Finally, Fig. 8 shows the reliability index for the Ultimate Limit State computed by either FORM and SORM techniques. Generally, we use the 20th order stochastic Taylor expansion technique, where some higher order components are postponed for lower order characteristics because they bring no additional contribution to the final result, so that the highest order expansion is treated as the exact result.

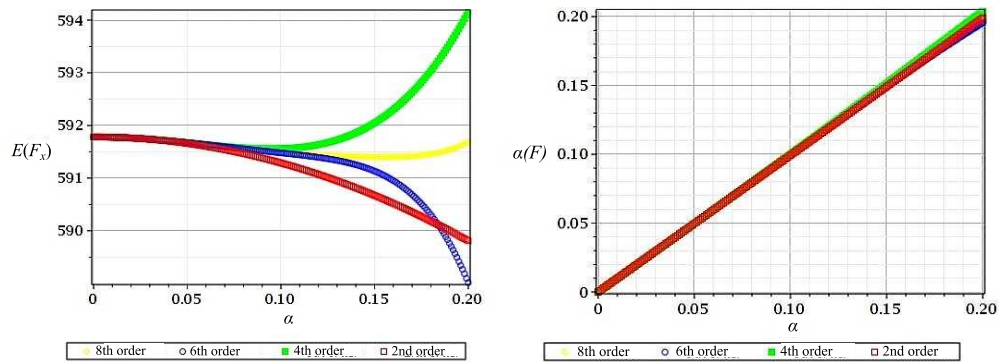


FIG. 6. Expected values (left) and variances (right) of the extreme normal force in the tower.

As one could expect, a relation of the extreme normal force in the tower after uniform and horizontal wind pressure almost linearly depends upon the mean wind speed, although we provide in further computations higher order poly-

mial as the approximation because it fits better the FEM data obtained. One may notice this structural system linearly depends upon the given external load even in geometrically nonlinear analysis including some geometrical imperfections and compliance of the supports. It can be noticed with a relatively small modelling error that Gaussian wind pressure induces Gaussian extreme normal force, which is decisive for the critical values ULS reliability index. This hypothesis is confirmed by further results, where the highest order approximations of the expected values are almost independent of the input coefficient of variation, where an output coefficient of variation almost linearly depends upon the input one and where skewness and kurtosis up to the certain level of the input $\alpha(\nu)$ remains 0 showing some numerical discrepancies for larger input uncertainty. It is worthy to underline that when one adopts a linear response function, then after the basic perturbation-based equations of any order for the probabilistic moments (see Eqs. (3.10)–(3.11)) the resulting expectation equals to the mean value and is constant, expansion for the variance reduces to the first term only, while skewness and kurtosis equal approximately zeroes, which contrasted with the above analysis validates this study. Quite typically for this method (cf. [23]) the odd central moments and characteristics (like skewness) exhibit less numerical stability than the even ones (including kurtosis). Skewness has very small negative values diverging systematically from 0, while kurtosis keeps zero up to the given level of the input randomness, see Fig. 7.

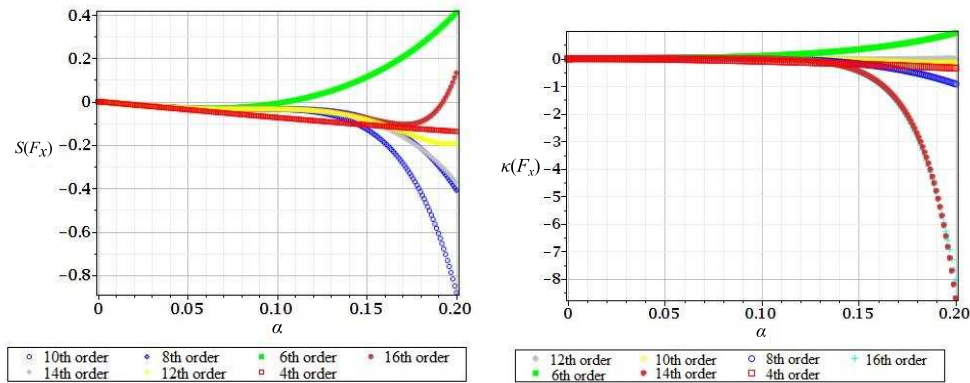


FIG. 7. Skewness (left) and kurtosis (right) of the extreme normal force in the tower.

Let us remind that determination of the examined tower reliability has been performed by using of the experimental data in the context of numerical model validation as well as the definition of the reliability indices (experimental values of the tower legs buckling resistances). The FEM model of the structure was created with respect to the supports susceptibility, geometrical imperfections and

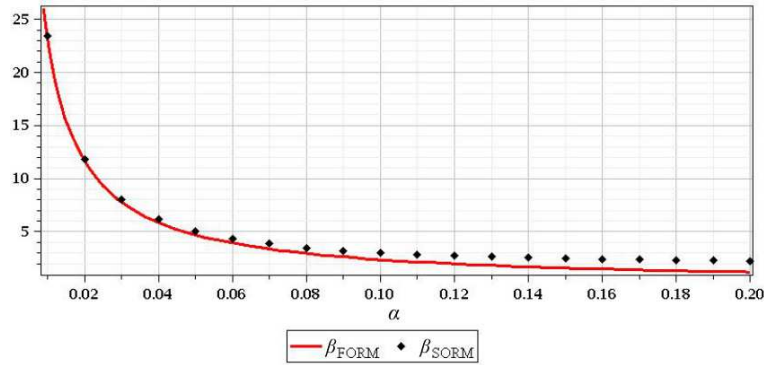


FIG. 8. Reliability index for the ULS (FORM, SORM) with respect to Gaussian random wind velocity.

material properties. In the reliability analysis mean wind velocity was treated as a Gaussian random variable. Figure 8 includes reliability indices (FORM, SORM) calculated for the tower – they are both given as the functions of the input wind velocity coefficient of variation α . Both indices traditionally decrease exponentially together with an increasing input random dispersion. Some differences in-between FORM and SORM have been noticed, which become apparent when $\alpha(\nu) > 0,05$ and where SORM returns a little bit larger values; additionally, this difference increases together with an input coefficient of variation. Nevertheless, all these differences are noticed for a reliability index having the value smaller than it is recommended by the civil engineering designing codes. It was decided to not discuss these aspects here.

5. Conclusions

The experimental-based Stochastic Finite Element Method analysis of the steel lattice tower presented in this paper shows clearly that the reliability of the considered structure is larger than it is suggested by the Eurocode demands. Similar studies related to the steel masts, chimneys, cable bridges and tall buildings would be recommended also. One of the most important results is that the Gaussian mean wind speed induces Gaussian extreme normal force being the basis for calculating of the ULS reliability index, so that an application of the FORM approach is well justified. This effect is obtained from both theoretical considerations following deterministic response functions (almost linear) and the resulting probabilistic characteristics. Let us note that this has been obtained for the geometrically nonlinear FEM structural analysis of the large scale structure implemented with the proposed scheme of SFEM, so that it may serve as some kind of validation of the stochastic perturbation method for nonlinear computer

analyses with uncertain loadings. A validity range of the higher order stochastic perturbation method in application to this kind of nonlinear problems has been given in accordance with the input coefficient of variation, which should be smaller or equal than 0.10. Skewness and kurtosis diverge from the theoretically justified values beyond this limit value, while the first two characteristics are almost insensitive to this limitation.

Further stochastic computational analysis should focus of course on stochastic dynamic excitations [24, 25] of these structures with the use of Taylor expansions of all the state functions and of the Least Squares Method approximations with the polynomial bases. Special attention should be paid to introduction of the shell finite elements discretization of the steel profiles to capture warping effect on the overall behavior of long structural elements under compression, better modeling of the joints [34], whose some specific stiffness may affect internal forces redistribution. Reliability based design optimization of the steel towers calibrated with the experimental results would be a very important and interesting issue similarly to the SFEM analysis of the aluminum tower structure contained in [35].

References

1. A. FLAGA, *Wind Engineering. Basis and Applications*, Warsaw, Poland, 2008 [in Polish].
2. B.W. SMITH, *Communication Structures*, Thomas Telford Publishing, London, 2007.
3. M. BELLOLI, Z. ROSA, A. ZASSO, *Wind loads on high slender tower: Numerical and experimental comparison*, *Engrg. Struct.*, **68**, 24–32, 2014.
4. C.F. CARRIL, N. ISYUMOV, M.L.R.F. REYOLANDO, *Experimental study of the wind forces rectangular latticed communication towers with antennas*, *J. Wind Engrg. & Industrial Aerodyn.*, **91**, 1007–1022, 2003.
5. P. MARTIN, V.B. ELENA, A.M. LOREDO-SOUZA, E.B. CAMAÑO, *Experimental study of the effects of dish antennas on the wind loading of telecommunication towers*, *J. Wind Engrg. & Ind. Aerodyn.*, **149**, 40–47, 2016.
6. J.D. HOLMES, *Along-wind response of lattice towers – I. Aerodynamic damping and deflections*, *Engrg. Struct.*, **18**, 7, 483–488, 1996.
7. J.D. HOLMES, *Along-wind response of lattice towers – II. Effective load distributions*, *Engrg. Struct.*, **18**, 7, 489–494, 1996.
8. F. ALBERMANI, S. KITIPORNCHAI, R.W.K. CHAN, *Failure analysis of transmission towers*, *Engrg. Failure Anal.*, **16**, 1922–1928, 2009.
9. R.N. PRASAD, G.M.S. KNIGHT, S.J. MOHAN, N. LAKSHMANAN, *Studies on failure of transmission line towers in testing*, *Engrg. Struct.*, **35**, 55–70, 2012.
10. C.H. NGUYEN, A. FREDI, G. SOLARI, F. TUBINO, *Aeroelastic instability and wind-excited response of complex lighting poles and antenna masts*, *Engrg. Struct.*, **85**, 264–276, 2015.
11. M.P. REPETTO, G. SOLARI, *Dynamic along wind fatigue of slender and vertical structures*, *Engrg. Struct.*, **23**, 1622–1633, 2001.

12. M.P. REPETTO, G. SOLARI, *Wind-induced fatigue collapse of real slender structures*, *Engrg. Struct.*, **32**, 3888–3898, 2010.
13. P.S. LEE, G. MCCLURE, *Elastoplastic large deformation analysis of a lattice steel tower structure and comparison with full-scale tests*, *J. Constr. Steel Res.*, **63**, 709–717, 2007.
14. J. SZAFRAN, *An experimental investigation into failure mechanism of a full-scale 40 m high telecommunication tower*, *Engrg. Failure Anal.*, **54**, 131–145, 2015.
15. J. SZAFRAN, K. RYKALUK, *A full-scale experiment of a lattice telecommunication tower under breaking load*, *J. Constr. Steel Res.*, **120**, 160–175, 2016.
16. S. KITIPORNCHAI, F. ALBERMANI, *Nonlinear finite element analysis of latticed transmission towers*, *Engrg. Struct.*, **15**, 259–269, 1993.
17. L. CARASSALE, G. SOLARI, *Monte Carlo simulations of wind velocity fields on complex structures*, *J. Wind Engrg. & Ind. Aerodyn.*, **94**, 323–339, 2006.
18. R. DEOLIYA, T.K. DATTA, *Reliability analysis of a microwave tower for fluctuating mean wind with directional effect*, *Rel. Engrg. & System Safety*, **67**, 257–267, 2000.
19. S. AU, J. BECK, *First excursion probabilities for linear systems by very efficient important sampling*, *Prob. Engrg. Mech.*, **16**, 193–207, 2001.
20. M. KAMIŃSKI, J. SZAFRAN, *Random eigenvibrations of elastic structures by the response function method and the generalized stochastic perturbation technique*, *Arch. Civil & Mech. Engrg.*, **9**, 4, 5–32, 2009.
21. M. KAMIŃSKI, J. SZAFRAN, *Stochastic finite elements analysis and reliability of steel telecommunication towers*, *CMES: Comput. Model. Engrg. & Sci.*, **2060**, 1, 1–25, 2009.
22. M. KLEIBER, T.D. HIEN, *The Stochastic Finite Element Method*, Wiley, Chichester, 1992.
23. M. KAMIŃSKI, *The Stochastic Perturbation Method for Computational Mechanics*, Wiley, Chichester, 2013.
24. L. KATAFYGIOTIS, S. CHEUNG, *Domain decomposition method for calculating the failure probability of linear dynamic systems subjected to Gaussian stochastic loads*, *J. Engrg. Mech.*, **132**, 5, 465–486, 2006.
25. B. GOLLER, H.J. PRADLWARTER, G.I. SCHÜLLER, *Reliability assessment in structural dynamics*, *J. Sound & Vibr.*, **332**, 2488–2499, 2013.
26. M. GIOFFRE, V. GUSELLA, M. GRIGORIU, *Non-Gaussian wind pressure on prismatic buildings. I: Stochastic field*, *J. Struct. Engrg.*, **127**, 9, 981–989, 2001.
27. *Autodesk Robot Structural Analysis User Manual*, Autodesk, 2015.
28. *Maple User Manual v. 2014*, Maplesoft, 2014.
29. Eurocode 3: Design of steel structures. Towers, masts and chimneys. Tower and masts. European Committee for Standardization, Brussels, 2008.
30. J SZAFRAN, Research experiment: <https://www.youtube.com/watch?v=AaVGCUEBoMw>.
31. G.A. YUAN, Z.A. WEI, *Limited memory BFGS method with backtracking for symmetric nonlinear equations*, *Math. & Comput. Model.*, **54**, 1, 2, 367–377, 2011.
32. G.A. YUAN, Z. WEI, Z. WANG, S.B. LU, *Gradient trust region algorithm with limited memory BFGS update for nonsmooth convex minimization*, *Comput. Optim. & Appl.*, **54**, 1, 45–64, 2013.

33. R.E. MELCHERS, *Structural Reliability Analysis and Prediction*, Wiley, Chichester, 1999.
34. W.Q. JIANG, Z.Q. WANG, G. MCCLURE, G.L. WANG, J.D. GENG, *Accurate modelling of joint effects in lattice transmission towers*, *Engrg. Struct.*, **33**, 1817–1827, 2011.
35. M. KAMIŃSKI, M. SOLECKA, *Optimization of the truss-type structures using the generalized perturbation-based Stochastic Finite Element Method*, *Finite Elem. Anal. & Design*, **63**, 69–79, 2013.

Received November 30, 2016; revised version April 7, 2017.
